TUTORIAL

A Comprehensive Framework for Physiologically-Based Pharmacokinetic Modeling in Matlab

Felix Stader[1,2,3,]*, Melissa A. Penny[2,3], Marco Siccardi[4] and Catia Marzolini[1,3]

Physiologically-based pharmacokinetic (PBPK) models are useful tools to predict clinical scenarios for special populations for whom there are high hurdles to conduct clinical trials such as children or the elderly. However, the coding of a PBPK model in a mathematical programming language can be challenging. This tutorial illustrates how to build a whole-body PBPK model in Matlab to answer specific pharmacological questions involving drug disposition and magnitudes of drug–drug interactions in different patient populations.

BACKGROUND

Physiologically-based pharmacokinetic (PBPK) models have been applied with significant impact during drug development and postmarketing phases and have achieved regulatory acceptance[1] as shown by the recent guidelines of the US Food and Drug Administration[2] and the European Medicines Agency.[3] PBPK models are useful for the prediction of drug–drug interaction (DDI) magnitudes[4] and drug disposition in special populations such as pediatrics,[5] pregnant and breastfeeding women,[6,7] and patients with liver cirrhosis[8] or renal impairment,[9] for all of whom there are high hurdles to design and conduct clinical trials. In addition, PBPK models have been successfully applied to simulate different routes of administration[10] and for the design of novel formulations.

A PBPK model describes the absorption, distribution, metabolism, and elimination of a drug in a physiologically relevant compartmental structure, where each compartment represents an organ or tissue.[11] The organs and tissues are connected via arteries and veins, which themselves merge in the lung. Dynamic drug movement through regional blood flows to the different organs and tissues is described by ordinary differential equations (ODEs). Tissue distribution can be predicted by a PBPK model that is of high relevance to most drugs because the drug targets are usually in specific populations of cells in an organ or tissue. The distribution into a compartment can either be limited by perfusion (well-stirred models) or by the cell membrane (permeability-limited models).[12]

An important characteristic of the PBPK modeling approach is the separation of system data (where the term *system* refers to the population of interest) from drug metabolism and pharmacokinetic data and the trial design.[12] System data contain all relevant information to build a population of virtual individuals such as demographics, organ weights, and regional blood flows. It is of tremendous importance

that the system data used to parameterize the PBPK system components reflects the "true" (meaning observed) population to produce reliable predictions.[13] The incorporated physiological, biochemical, and genetic variability of system parameters allows the identification of certain subpopulations with high risks for DDIs (e.g., poor metabolizers for the enzyme cytochrome P450 (CYP) 2D6), where clinical data are often lacking.[14] However, variability is often underestimated in PBPK models because of missing parameters or processes involved with physiological changes caused by diseases or specific patient characteristics, all of which add uncertainty and variability.[15]

Drug metabolism and pharmacokinetic data describe the information related to physicochemical properties (e.g., molecular weight), absorption (e.g., intestinal permeability), distribution (e.g., binding to plasma proteins), metabolism (e.g., kinetic parameters for an enzyme), and excretion (e.g., renal clearance).[16] Usually drug characteristics, such as the intrinsic clearance of an enzyme, are quantified through laboratory-based experiments that are then scaled to the *in vivo* clearance under the consideration of system parameters such as the enzyme abundance in the liver per gram protein, the protein content per gram liver, the liver weight, and the hepatic blood flow.[17] By considering variability in these system parameters, it is possible to obtain reliable population predictions of drug clearance.[14] System and drug data can be combined in the trial design component, considering parameters such as dose, dosing regimen, route of administration, number of individuals, and duration of administration to simulate clinical scenarios of interest.

Several commercial PBPK software platforms, such as SimCYP,[18] PK-Sim,[19] and GastroPlus[20] simplify the model management for unexperienced modelers and are based on structural PBPK models. However, they are limited in flexibility to simulate specific pharmacological questions. In this tutorial, a general framework on how to build a whole-body PBPK model in Matlab (MathWorks, Natick, MA) is

[1]Division of Infectious Diseases and Hospital Epidemiology, Departments of Medicine and Clinical Research, University Hospital Basel, Basel, Switzerland; [2]Infectious Disease Modelling Unit, Department of Epidemiology and Public Health, Swiss Tropical and Public Health Institute, Basel, Switzerland; [3]University of Basel, Basel, Switzerland; [4]Department of Molecular and Clinical Pharmacology, Institute of Translational Medicine, University of Liverpool, Liverpool, UK. *Correspondence: Felix Stader (felix.stader@unibas.ch)

described for scientists and users with interest in mathematical modeling and its application in pharmacology. The general development can also be adapted in other programming languages such as R or other Matlab packages such as Simbiology.

FIVE STEPS TO BUILD A PBPK MODEL IN MATLAB

Matlab offers a powerful mathematical programming language with matrix-based operations (https://uk.mathworks.com/products/matlab.html). The basic principles of Matlab are extensively described in the documentation by MathWorks (https://uk.mathworks.com/help/matlab/index.html). This tutorial illustrates the different steps necessary to build a PBPK model to simulate specific clinical scenarios with examples of pseudo code separated by lines from the main text. The entire code and tables listing the abbreviation and units for all used parameters can be found in the supplement (**Tables S1 and S2**). The Statistic and Machine Learning Toolbox is a required Add-On to the Matlab suite to execute the code.

A "building block" system is used for separating system, drug, and trial design data to inform the PBPK model.[12] The advantages are that each block can be used for a different purpose (e.g., the generated population could be used in a different model), and each block can be exchanged (e.g., aging white population vs. pediatric population[21]). Each building block described in this tutorial is a Matlab function. Matlab requires one script indicating the order in which the functions should be executed, which in this tutorial is called the main function.

```
%Main function: Calls each function of a
PBPK model

Define the model structure and the model
parameters
Generation of the virtual population
Load the drug files and perform the in vitro
to in vivo extrapolation
solve the ordinary differential equations
(ODEs)
process the data from the ODE solution and
output the results
```

The variables used in different functions in Matlab need either to be passed onto the next function or to be defined as globals using the "global" command. However, it is good practice to scope variables as local if they are only used within a specific script.

Step 1: Define the parameters of the model
The modeling process is started by defining the objective and the purpose of the model, identifying the pharmacological scenario to be simulated. The model structure proposed can vary based on the overall purpose of the simulations, and a representative compartmental model is shown in **Figure 1**.[22] As an example, it would be of scientific interest to simulate clinical scenarios in aging HIV-infected patients because clinical data of antiretroviral drug disposition and DDI magnitudes between antiretroviral agents and comedications are currently lacking. When simulating anti-HIV therapy, drug penetration into viral reservoirs, such as the testis and the brain,[23] and into the lymphatic system being the target site for antiretroviral drugs can represent a relevant pharmacokinetic factor. The flexible computational structure supports the inclusion of the lymphatic system, dividing each compartment into the vascular, interstitial, and intracellular spaces (**Figure 2**) with lymph fluid flowing from the interstitial space of each organ to a central lymph-node compartment and further to the venous blood pool. Organs not being simulated are lumped into a remaining organ compartment.[13] In our example, the model is used to simulate the effect of the CYP3A4 inhibitor ritonavir, used as a pharmacokinetic enhancer to boost the concentrations of coadministered HIV protease inhibitors such as darunavir, on the disposition of the anticoagulant rivaroxaban being metabolized by CYP3A4 in aging white subjects.

First, the model structure and model variables, including populations, compartments, drugs, and routes of administration are defined by a number because Matlab is a numerical software tool. The number assigned to each variable (e.g., drugs) refers to the column in each matrix containing specific data (e.g., if darunavir is defined by a one, the data of darunavir would be in the first column; **Figure 3**). Each variable is also defined by a string defining its name for the outputs.

After defining all necessary variables of the model, the target population and the drugs to be used in a specific simulation need to be entered. The virtual trial design can be described by first indicating the number of virtual individuals in the simulation. The appropriate number of individuals depends on the variability of system data involved to describe the pharmacokinetics of the simulated drug (e.g., enzymatic vs. total clearance) and the number of patients included in clinical trials to verify the model. To come to the "true" population mean for most anatomical, physiological, and biological parameters, a sample size of at least 100 individuals is recommended. Of note, for system parameters with high variability, such as enzyme and transporter abundance, a virtual population containing 500 individuals might be more appropriate.[24] Therefore, if observed clinical data are available for six patients, it is recommended to run 20 trials times six patients, resulting in 120 virtual individuals. The split into different trials allows the comparison of the mean predicted concentration of each trial with the mean observed data. The mean observed is used because often observed concentration from individuals are not published or available. Observed data from six individuals may not be representative of the whole patient population taking the drug of interest; thus, it is important to recognize that the mean prediction obtained might be different and far from the mean of the six observed subjects, but it might be close to the "true" population of patients. Therefore, if the observed data from six subjects fit the prediction of one trial, even when its prediction should be on the upper or lower end of all simulations, this is still considered to be a "successful" outcome.

Next the proportion of men and women in the simulated population and the age range of the virtual individuals can be specified. In addition, the resolution of each simulated time unit needs to be given for the outputs.
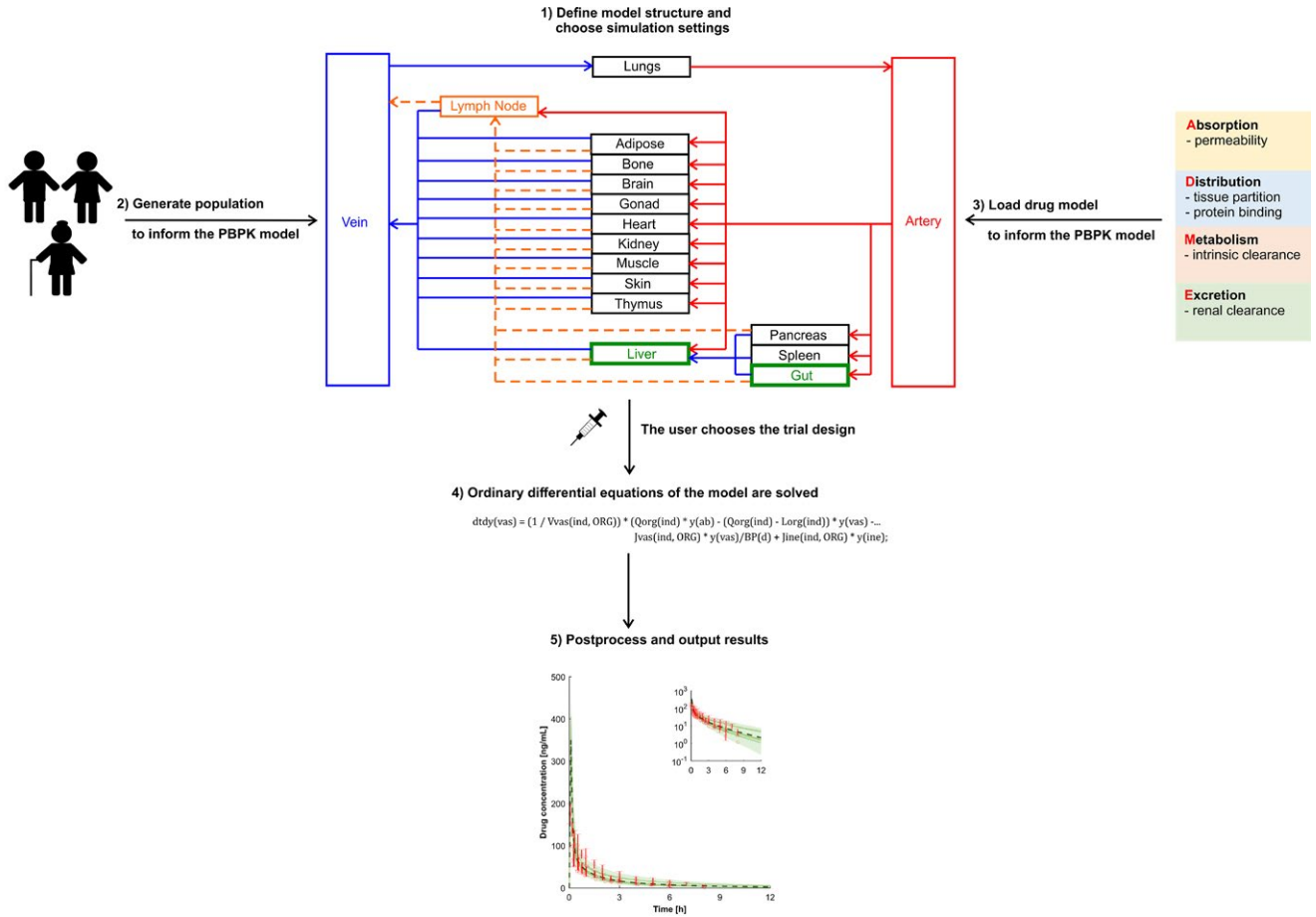
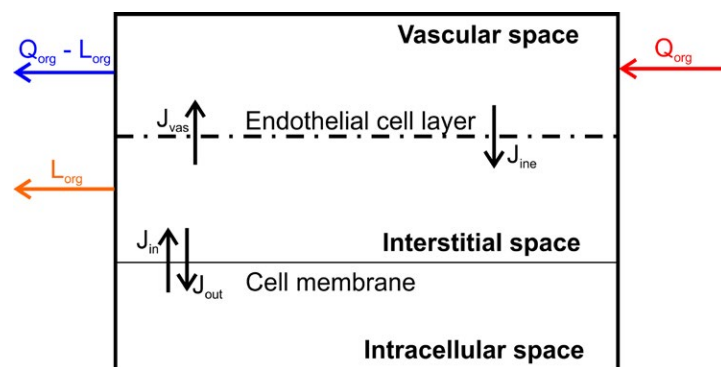**Figure 1** Schematic illustration of the five steps to build a physiologically-based pharmacokinetic model.

Figure 2 Structure of an organ in the model. J_{in}, flux into the cell; J_{ine}, flux from the interstitial to the vascular space; J_{out}, flux out of the cell; J_{vas}, flux from the vascular to the interstitial space; L_{org}, regional lymph flow; Q_{org}, regional blood flow.

Once the individual characteristics are described, the dosing regimen for each drug can be defined, indicating the route of administration, the number of doses (1 for a single dose and *n* for multiple doses), the dose, and the dosing interval. After entering the trial design, a dose event matrix can be set up to allow the simultaneous simulations of darunavir, ritonavir, and rivaroxaban alone and in combination to investigate DDIs. The matrix contains five columns with the start and the end time of each dose, the dose, the route of administration, and the resolution for each dosing event. Only unique start and end times for each dosing event are needed, which need to be extracted.
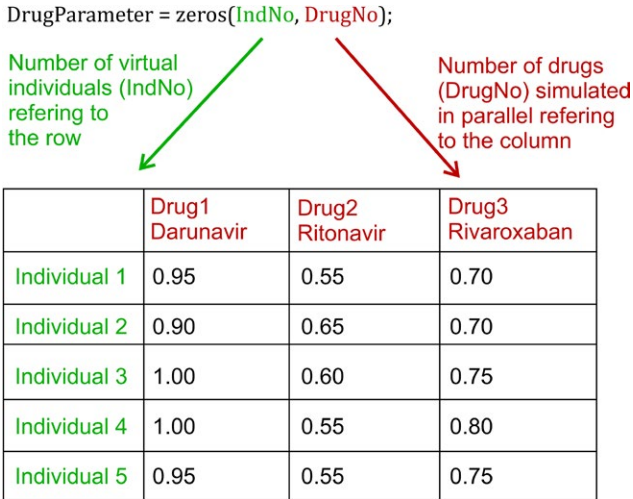
```
DrugParameter = zeros(IndNo, DrugNo);
```

Number of virtual individuals (IndNo) refering to the row

Number of drugs (DrugNo) simulated in parallel refering to the column

	Drug1 Darunavir	Drug2 Ritonavir	Drug3 Rivaroxaban
Individual 1	0.95	0.55	0.70
Individual 2	0.90	0.65	0.70
Individual 3	1.00	0.60	0.75
Individual 4	1.00	0.55	0.80
Individual 5	0.95	0.55	0.75

Figure 3 Example of the organization of drug parameters with variability. Each row contains data for an individual, and each column contains data for a drug. Parameter clues are illustrative only. IndNo, number of virtual individuals. DrugNo, number of drugs.

The code to define the model parameters and choose the simulation settings is given by:

```
function[] = DefineParameters()

%This function defines the population,
model structure (PBPK compartments),
%the drugs, the virtual trial design and
the simulation settings to be used

%==========================================
===============

Define the populations saved on the hard
drive by a number and a string

Define the compartments of the model by a
number and a string
Define enzymes for the dynamic abundance
calculation in case of DDIs by a number and
a string
Define the number of subcompartments

Define the drugs saved on the hard drive by
a number and a string
Define plasma-binding proteins by a number
and a string

Define the route of administration by a
number and a string

%==========================================
===============

User sets the population to be simulated (if
more than one is saved on the hard drive)
```

```
User sets the number of drugs to be simulated
Initialize drug name

Define a case for each simulated drug
        define a drug name for each drug to
        be simulated
end

Define the number of trials
Define the number of virtual individuals
per trial
Calculate the number of all virtual
individuals to be simulated

Ask the user for the proportion of women in
the virtual population
Ask the user for the minimal and maximal age
of the virtual population to be simulated

Ask the user for the resolution of each
time step

Initialize the route of administration,
the number of doses, the dose, the dose
interval, the start timepoint for the
dose, and the prolongation of the terminal
elimination phase.

Define a case for each drug to be simulated
        Define the route of administration
        to be an iv bolus or oral
        Define the number of doses and dose
        given in mg
        Define the dose interval in h
        Set a start time for the drug to be
        administered in h
        Set the prolongation for the
        terminal elimination phase in h
end

%==========================================
===============

Define the name of the columns for the dose
event matrix
Calculate the number of columns of the dose
event matrix

Initialize a matrix containing the regimen
for each drug
Define a case for each drug
        Define a case for each dose being
        administered
            Calculate the start time for the
            first dosing event
            Calculate the end time for the
            first dosing event

            Calculate the start time for all
            dosing events
```

```
        Calculate the end time for all
        dosing events

        Consider the prolongation of the
        terminal elimination phase
      end
end

Define a case for each drug
      sort the regimen matrix based on the
      start time of each drug
      delete zero values
end

Define a case for each drug
      combine the dosing regimens for
      different drugs
      use a function to find unique dosing
      events for each drug
            set dose, route of
            administration, and resolution
            for the other drugs to be zero
            sort the matrix according to the
            start time
            find unique start times
            output the dose event matrix for
            each drug based on the unique
            start times
      end
end

Calculate the number of events
Put together the dose event matrix

end
```

Step 2: Generation of the population

A repository summarizing the anatomical, physiological, and biological system parameters required to inform a PBPK model has been recently published.[13] The described continuous, age-dependent equations and the variability for each system parameter can be directly entered in Matlab:

```
function[] = Population()

%This function generates the virtual
population based on the user settings
%Attention: the normrnd command needs the
Statistics and Machine Learning Toolbox

Calculate age from a Weibull distribution
for each virtual individual
      while age of an individual is smaller
      or larger than the minimal or maximal
      user-defined age
            Resample age from the Weibull
            distribution
```

```
      end
end

Calculate number of virtual female
individuals
Assign randomly a zero (defined as "male")
or one (defined as "female") to each virtual
subject

Calculate system parameters as described in
ref: [13]
Add random variability to the system
parameters by using a normal described

end
```

Step 3: Calculation of the required drug parameters

In the next step, the user-defined drug file is loaded from the library containing all developed drug files. The string defining the drug (e.g., "darunavir") is converted to the function in the drug library to load the drug-dependent data to inform the PBPK model (**Figure 4**):

```
function[] = Drug()

%This function loads the relevant drug files
from the drug library and
%performs the in vitro-to-in vivo
extrapolation

Define a case for each drug
      load the Matlab file containing the
      drug parameter by converting the
      string defining the…
      drug to the function in the drug
      library
end

end
```

Drug parameters incorporated in a drug file are shown in **Table 1**. The measured drug properties included in the drug file can be derived through experimental *in vitro* methods and integrated into specific equations for drug absorption, distribution, and elimination as described in the following sections.

Absorption. The compartmental absorption and transit model proposed by Yu and Amidon[25] about 20 years ago is used as a basis. The assumptions of the original compartmental absorption and transit model are the following:

1. The drug is immediately dissolved
2. Absorption occurs primarily in the small intestine and not in the stomach or the colon
3. Transit time and radii are similar for each compartment
4. Intestinal metabolism is negligible
5. Only passive diffusion occurs through the gut wall

1) Define the drug as a variable

Darunavir = 1;   name{darunavir} = ‚darunavir';

2) Convert the string ‚darunavir' to the function „darunavir" to load drug data for darunavir

Drug1 = str2func(name{darunavir});
Drug1();

3) Data from the drug model darunavir saved in the function „darunavir" are used

function[ ] = darunavir

%__PhysChem_____
%molecular weight (MW) in g/mol
MW(darunavir)   = 547.7;   %Molto et al. (2016)

%octanol-water partition coefficient (logP)
logP(darunavir)   = 1.8;%   %Molto et al. (2016)

Figure 4 Steps from the user-defined drug to be simulated to the drug parameter that are loaded to inform the physiologically-based pharmacokinetic model.

It can be assumed that assumption 1 holds true for antiretroviral drugs because they are often given as an immediate-release tablet. Formulation and dissolution play a crucial role when simulating capsules or delayed-release tablets, and more complex absorption models can be built into the model as previously described.[26,27] The compartmental absorption and transit model consists of five different compartments, namely, the stomach, duodenum, jejunum, ileum, and colon. The stomach serves as an entry compartment for the orally administered drug. It is assumed that the drug can only move further to the duodenum and no absorption or other processes occur in the stomach. Movement between different compartments representing the intestine can be described by first-order rate constants calculated from the gastric emptying and the intestinal transit time.[25]

Permeability into enterocytes and further into the systemic circulation can be mediated by passive or active processes. Drug transporters are present on the apical and basolateral site of the small intestine.[28] An established experimental model such as human epithelial colorectal adenocarcinoma cells seeded as a monolayer can be used to measure the apparent permeability (P_{app}) *in vitro* and depending on the experimental conditions, the measured flux into the cell can be the sum of passive and active. The measured P_{app} can be converted to the effective permeability in man ($P_{eff,man}$) describing the flux of the drug from the lumen into the enterocytes in humans[29] as follows:

$$P_{eff,man} = 10^{0.6795*\log(P_{app})-0.3355}, \quad (1)$$

where P_{app} is in 10^{-6} cm/s and $P_{eff,man}$ is in 10^{-4} cm/s. $P_{eff,man}$ needs to be multiplied by the available enterocyte surface for drug absorption (permability surface area PSA) to arrive at the absorption clearance (CL_{ab}) (please note that the flux between two compartments can be written as a clearance), namely:

$$CL_{ab} = P_{eff,man} * PSA * 0.001 * 3,600 \quad (2)$$

where CL_{ab} is in L/h. The PSA can be calculated by assuming that the gut has a cylindric shape, namely:

$$PSA = 2 * \pi * r * Le * F_{Villi} \quad (3)$$

where r is the radius of each intestinal segment in centimeters, Le is the length of each intestinal segment in centimeters, and F_{villi} is a fold expansion factor for the villi surface area. The length and the expansion factors for the different gastrointestinal segments has been extensively described previously.[30,31] Drugs penetrate through the intestinal wall mainly by the transcellular pathway because of the tight junctions between enterocytes. Paracellular transport is only possible for drugs with a molecular weight <300 Da being positively charged and with an octanol-water partition coefficient (log$P$) > 0.[32]

Table 1 Parameters required for a drug file to inform the physiologically-based pharmacokinetic model

Parameter	Typical units	Explanation
Physicochemical properties		
MW	g/mol	Molecular weight
log*P*	–	Octanol-water partition coefficient
Compound type	–	Important property to predict tissue distribution according to Rodgers and Rowland
pKa	–	Acid dissociation constant
BP	–	Blood-to-plasma ratio
fu$_{PL}$	–	Fraction unbound in plasma
Absorption		
P_{app}	×10^{-6} cm/s	Apparent permeability
Distribution		
Kp scalar	–	Scalar to alter predicted partition coefficient
Elimination		
V_{max}/K_m or CL$_{int}$	pmol/minute/pmol enzyme/μM or μmol/minute/mg protein	Kinetic parameters per enzyme and metabolic pathway
CL$_r$	L/h	Renal clearance
CL$_{ad}$	L/h	Additional plasma clearance
Transporter		
CL$_{pd}$	μL/minute/Mio cells	Passive diffusion flux
V_{max}/K_m or CL$_{int}$	pmol/minute/pmol transporter/μM or μmol/minute/Mio cells	Kinetic parameters for transporters
Interactions		
K_i	μM	Inhibition constant for competitive inhibition
K_{app}	μM	Apparent enzyme inhibition constant for mechanism-based inhibition
k_{inact}	1/h	Maximum inactivation rate constant
IndMax	–	Maximum fold of induction
IC$_{50}$	μM	Half maximum inhibitory concentration

To estimate the concentration in the enterocyte, the volume of the enterocytic cell layer needs to be determined. A jejunal biopsy was undertaken in 11 healthy controls (five women) aged younger than 30 years, and 3,040 enterocytes were found in the sample. The volume of one enterocyte is 770 μm^3, calculated as a cylinder from the measured height and radius.[33] The surface of the small intestine can be calculated by assuming a cylindric shape and the radius and length of 2.25 cm and 280/260 cm for an average male/female subject, respectively.[31] The resulting surface area of the small intestine is 3,958/3,676 cm^2. Scaling the number of enterocytes from the biopsy sample to the entire small intestine leads to $1.20 \times 10^{11}/1.12 \times 10^{11}$ cells. The total volume of all enterocytes in the small intestine is therefore 0.093/0.086 L.

The drug distributes further from the enterocytes to the interstitial space and could move further either via the systemic or the lymphatic circulation. The potential strategies for antiretroviral drugs include manipulating the formulation in such a way so that more drug gains access into the lymphatic system because (i) it is the relevant target site, (ii) there will be no first-pass metabolism, and (iii) the drug stays longer in the body because intestinal lymph flow is about 600-fold slower than intestinal blood flow.[31,34] To move preferentially into the lymph circulation rather than into the systemic circulation, a drug needs to be highly lipophilic and positively charged and should have a high molecular weight.[35] However, there are no quantitative relationships in the literature. A manual restriction factor can be implemented into the model defining a proportion of the drug going via the lymphatic system to test new formulations. The rest of the drug will distribute via systemic circulation.

Distribution—passive and active pathways. The prediction of tissue distribution is important in a PBPK model. Intracellular concentrations cannot be easily obtained, particularly in humans, but most drug targets are in cells. In addition, metabolism occurs in hepatocytes and enterocytes, and therefore intracellular concentration is important to predict metabolism and DDI magnitudes adequately. Several models are described in the literature to predict distribution into tissue.[36–41] Poulin and Theil[36,37] assume homogenous distribution in a tissue, which does not hold true if the cell membrane is a tight barrier. Therefore, the approach of Rodgers *et al*.[38] and Rodgers and Rowland[39,40] is used in this model. In contrast to Poulin and Theil, Rodgers *et al*. consider binding to different constituents of the cell, such as lipids and proteins.

Calculation of partition coefficients. Mono protic- and diprotic basic drugs with an acid dissociation constant > 7 interact preferentially with acidic phospholipids in the tissue through electrostatic interactions. Binding to extracellular proteins may not play an important role because basic drugs preferentially bind to alpha-acidic glycoprotein, which is mostly restricted to plasma. Therefore, an affinity constant for acidic phospholipids (KaAP) is calculated for red blood cells. The partition coefficient for the unbound drug into red blood cells can be calculated from the blood-to-plasma (BP) ratio, which itself can be measured *in vitro*. It is assumed that KaAP is similar for all tissues. Generally, the tissue partition coefficient of the unbound drug (Kpu) for muscle should be preferred as there is a good correlation between distribution into muscle and distribution into other tissues. The unbound drug partition coefficient for erythrocytes is given by ref. 38:

$$\mathrm{Kpu}_{RBC} = \frac{C_{RBC}}{C_{PL} * \mathrm{fu}_{PL}} = \frac{BP * HCT + (1 - HCT)}{\mathrm{fu}_{PL}} \quad (4)$$

where C = concentration, fu = fraction unbound in plasma, HCT = hematocrit, PL = plasma, and RBC = red blood cells. The affinity constant for acidic phospholipids is given by ref. 38:

$$KaAP_{RBC} = \left[Kpu_{RBC} - \left(\left(\frac{K_{io,RBC}}{K_{io,PL}}\right)*f_{IW,RBC}\right) \right.$$
$$- \left(\frac{\log P*f_{NL,RBC}+(0.3*\log P+0.7)*f_{NP,RBC}}{K_{io,PL}}\right)\right] \qquad (5)$$
$$\left. *\left[\frac{K_{io,PL}}{[AP]_{RBC}*(K_{io,RBC}-1)}\right]\right]$$

$$Kpu_{org} =$$
$$\left(\frac{K_{io,IW}*f_{IW,org}}{K_{io,PL}}\right)+f_{EW,org}+\left(\frac{KaAP_{RBC}*[AP]_{org}*(K_{io,IW}-1)}{K_{io,PL}}\right)$$
$$+\left(\frac{\log P*f_{NL,org}+(0.3*\log P+0.7)*f_{NP,org}}{K_{io,PL}}\right) \qquad (6)$$

where K_{io} = ionized form according to Henderson-Hasselbalch,[39] f_{IW} = fraction of intracellular water, f_{EW} = fraction of extracellular water, f_{NL} = fraction of neutral lipids, f_{NP} = fraction of neutral phospholipids, and AP = acidic phospholipids. The subscript org represents organ. For the partitioning into the adipose tissue, it is more accurate to use the vegetable oil:water partition coefficient ($\log D_{vo:w}$) rather than $\log P$, namely[36]:

$$\log D_{vo:w} = (1.115*\log P - 1.35) - \log(K_{io,PL}) \qquad (7)$$

Binding to extracellular albumin should be considered for drugs that are not moderate to strong bases thus requiring the determination of the affinity constant for binding proteins (KaPR). The calculation is done for plasma because albumin concentration in plasma is known, and the unbound fraction in plasma can be determined in *in vitro* experiments. It is assumed that $KaPR_{PL}$ holds true for all tissues,[39] namely:

$$KaPR_{PL} =$$
$$\left[\frac{1}{fu_{PL}}-1-\left(\frac{\log P*f_{NL,PL}+(0.3*\log P+0.7)*f_{NP,PL}}{K_{io,PL}}\right)\right]*\frac{1}{PR_{PL}} \qquad (8)$$

where PR_{PL} is the binding protein concentration in plasma in g/L. The unbound drug partition coefficient is given by ref. [39]:

$$Kpu_{org} = \left(\frac{K_{io,IW}*f_{IW,org}}{K_{io,PL}}\right)+f_{EW,org}+(KaPR_{PL}*KpPR_{org}*PR_{PL})$$
$$+\left(\frac{\log P*f_{NL,org}+(0.3*\log P+0.7)*f_{NP,org}}{K_{io,PL}}\right) \qquad (9)$$

where $KpPR_{org}$ is the partition coefficient of plasma-binding proteins in different organs.

The apparent volume of distribution in steady state (V_{ss}) can be calculated as follows[40]:

$$V_{ss} = \frac{V_{PL}}{fu_{PL}}+\sum V_{org}*Kp_{org} \qquad (10)$$

where V is the volume and Kp is the total tissue partition coefficient, which is defined as[38]:

$$Kp = \frac{C_{org}}{C_{PL}} = fu*Kpu. \qquad (11)$$

A Kp scalar can be introduced to the model, which multiplies the predicted Kp

$$Kp_{used} = Kp*Kp\ scalar \qquad (12)$$

and can be used to correct for insufficient tissue partition prediction. One such example is the extensive lysosomal trapping or binding to intracellular constituents such as DNA (e.g., doxorubicin).[38]

When splitting every compartment of the PBPK model into the subcompartment vascular, interstitial, and intracellular spaces, the distribution through the endothelial cell layer and through the cell membrane are required to inform the PBPK model. The endothelial cell layer is not a tight barrier for small molecule drugs, thus it can be assumed that the extracellular water is almost instantaneously in equilibrium. Under physiological conditions, blood comes with high pressure into the capillaries, and its content is pushed against the endothelial cell layer and through the small and large pores into the interstitial space.[42] There is a partial fluid loss, the lymph, which is recycled back to the venous blood pool via the lymph nodes. Erythrocytes cannot cross the endothelial cell layer, and hence the lymph is colorless.

The calculated Kp is used to estimate the flux through the cell membrane between the interstitial and the intracellular spaces, when experimental data about cell membrane permeability are not available. It holds true that the concentration in plasma equals the concentration in the vascular space, which is considered to belong to the blood, namely:

$$Kp = \frac{C_{org}}{C_{PL}} = \frac{C_{ine}+C_{cel}}{C_{vas}} = \frac{C_{ine}}{C_{vas}}+\frac{C_{cel}}{C_{vas}} \qquad (13)$$

where the subscripts vas, ine, and cel represent vascular, interstitial and intracellular, respectively. Kp is determined in steady state and under steady-state conditions, the vascular and interstitial space concentration differ by the drug concentration in erythrocytes, and the interstitial and intracellular drug concentration differ by the fraction unbound and the flux through the membrane, namely:

$$Kp = \frac{1}{BP}+\frac{J_{in}*fu_{ine}}{J_{out}*fu_{cel}}. \qquad (14)$$

Kp can only be described by the ratio of influx (J_{in}) and efflux (J_{out}) of the cell.

Fraction unbound in the interstitial and intracellular spaces. A critical parameter for the distribution of a drug is fu in each compartment. Usually, fu is only measured in plasma samples, but the site of metabolism or efflux transporters is intracellular, making it necessary to know fu_{cel}. In a first step, the age dependency of fu is calculated for each virtual individual based on the measured fu *in vitro* and the main binding protein. "Ref" refers to a 30-year-old adult who is arbitrarily used to represent a "young" subject. It is assumed that the binding affinity does not change with age, and therefore fu for plasma is given by ref. 9:

$$fu_{PL} = \frac{1}{1+PR_{PL}*\left(\frac{\frac{1}{fu_{Ref}}-1}{PR_{PL,Ref}}\right)}. \qquad (15)$$

In a second step, fu in the interstitial space of each organ is estimated based on the known partition coefficient for the plasma-binding proteins in each tissue.[38] It is assumed that the binding affinity is the same as in plasma. Thus, fu_{ine} is calculated as follows:

$$fu_{ine,org} = \frac{1}{\frac{KpPR_{org}}{f_{EW,org}} * \left(\frac{1}{fu_{PL}} - 1 \right) + 1}. \tag{16}$$

fu_{cel} is calculated according to Rodgers and Rowland,[39] namely:

$$fu_{cel,org} = \frac{1}{1 + \left[\left(\frac{logP * f_{NL,org} + (0.3 * logP + 0.7) * f_{NP,org}}{K_{io,PL}} \right) + KpPR_{org} * PR_{PL} \right]}. \tag{17}$$

Active drug transporters. Drug transporters can theoretically be implemented into any compartment of the model to represent active distribution into cells, but absolute transporter abundance values to inform the PBPK model are only available for the liver.[43] There are some important points to consider before implementing a transporter into a PBPK model. Each transporter has a direction, and its impact will depend on whether the transporter is expressed on the apical or basolateral site. Passive permeability can occur besides active transport for given compounds, and therefore it is important to define the contribution of each of these transport processes. The overall contribution of uptake transporter is likely to be negligible for compounds characterized by a high passive permeability. Conversely, efflux transporters will have a pronounced impact for compounds characterized by a slow passive diffusion. Importantly, uptake and efflux transporters are exposed to different drug concentrations and thus the unbound drug concentration in the interstitial and intracellular spaces should be used for uptake and efflux transporters, respectively.[44] Transporter functionality can be described by Michaelis–Menten kinetics; however, $V_{max,T}/K_{m,T} = CL_{u,int,T}$,[45] where $V_{max,T}$ is the maximum transport rate, $K_{m,T}$ is the Michaelis–Menten constant for a transporter, and $CL_{u,int,T}$ is the intrinsic transport clearance of the unbound drug, only holds true if the unbound concentration is much smaller than K_m (fu x $C \ll K_m$). This is the case under physiological conditions in the cell but might not hold true for uptake transporters being exposed to the interstitial concentration. In addition, Michaelis–Menten assume one binding site per transporter, which is questionable, for instance, for the organic anion-transporting polypeptide 1B1.[46] Active hepatic drug transporters can be described by ref. 45:

$$CL_{int,T,tot,hep} = \left[\sum_{u=1}^{m} \left(\left(\frac{V_{max,up,hep,u}}{K_{m,up,hep,u} + C_{ine} * fu_{ine}} + CL_{int,up,hep,u} \right) * AB_{up,hep,u} \right) - \sum_{e=1}^{m} \left(\left(\frac{V_{max,ef,hep,e}}{K_{m,ef,hep,e} + C_{cel} * fu_{cel}} + CL_{int,ef,hep,e} \right) * AB_{ef,hep,e} \right) \right] * HPGL * liver weight \tag{18}$$

where HPGL is the hepatocellularity, and AB is the abundance. The subscripts T, tot, hep, up, eff, u, and e stand for

transporter, total, hepatic, uptake, efflux, uptake, and efflux transporter isoform, respectively.

Metabolism and elimination. The following four different options are described to represent drug clearance in the model:

1. Enzymatic intrinsic clearance
2. Intrinsic hepatic clearance not assigned to a specific enzyme
3. Renal clearance
4. Additional plasma clearance

Enzymatic intrinsic clearance can be either represented as $CL_{int,E}$ or through $V_{max,E}$ and $K_{m,E}$, where $CL_{int,E}$ is the intrinsic clearance, $V_{max,E}$ is the maximum metabolism rate for each enzyme, and $K_{m,E}$ is the Michaelis–Menten constant for each enzyme. Different pathways can be implemented considering active metabolic pathways,[47] namely:

$$CL_{int,E,tot,hep} = \sum_{j=1}^{J} \left(\sum_{i=1}^{I} \left(\left(\frac{V_{maxE,hep,j,i}}{Km_{E,hep,j,i}} \right) + CLint_{E,hep,j,i} \right) * AB_{E,hep,j} \right) * MPPGL * liver weight \tag{19}$$

$$CL_{int,E,tot,gut} = \left[\sum_{j=1}^{J} \left(\sum_{i=1}^{I} \left(\left(\frac{V_{maxE,gut,j,i}}{K_{mE,gut,j,i}} \right) + CL_{int,E,gut,j,i} * AB_{E,gut,j} \right) \right) \right] \tag{20}$$

where MPPGL is the microsomal protein per gram liver. The subscript E stands for enzyme, i stands for the metabolic pathway, and j represents the enzyme isoform.

The intrinsic hepatic clearance not assigned to a specific enzyme has the units μmol/minute/mg and is scaled via MPPGL and liver weight but not CYP abundance (which is not a problem for geriatric but would be for Japanese, pediatrics, etc.), namely:

$$CL_{int,tot,hep} = CL_{int,E,tot,hep} + CL_{int,hep} * MPPGL * liver weight. \tag{21}$$

The well-stirred liver model is used to calculate the hepatic clearance from the intrinsic clearance[48] and is given by:

$$CL_{hep} = \frac{Q_{LI} * fu_{BL} * CL_{int,tot,LI}}{Q_{LI} + fu_{BL} * CL_{int,tot,LI}} \tag{22}$$

where CL_{hep} is the total hepatic clearance in L/h, Q_{LI} is the hepatic blood flow, and fu_{BL} is the fraction unbound in blood.

The renal clearance is scaled via the glomerular filtration rate (GFR) and ignores tubular secretion and active transport processes, which would require a more mechanistic PBPK model[49] and is given by[50]:

$$CL_R = CL_{R,Ref} * \frac{GFR}{GFR_{Ref}} * \frac{fu}{fu_{Ref}}, \quad (23)$$

where CL_R is the renal clearance in L/h.

The fourth clearance option in the PBPK model is the additional plasma clearance (CL_{ad}). This parameter is always used as a fixed value, not scaled to any population, but it offers the possibility to enter an *in vivo* clearance value if clearance mechanism pathways are completely unknown. In cases when there are no measured *in vitro* values for enzymatic kinetic parameters or $CL_{int,tot,hep}$ but the *in vivo* clearance and the different contributions of metabolism and elimination pathways are known, a retrograde calculation can be performed to inform the PBPK model.[51]

The total clearance can be written as follows:

$$CL_{tot} = \frac{Q_{LI} * fu_{BL} * CL_{int,tot,LI}}{Q_{LI} + fu_{BL} * CL_{int,tot,LI}} + CL_R + CL_{ad}. \quad (24)$$

DDI. The PBPK framework allows simulation of competitive inhibition (whereby the inhibitor binds to the active site of the enzymes and blocks its activity), mechanism-based inhibition (whereby the inhibitor represses the transcription or translation of the metabolizing enzyme leading to a loss of enzyme concentration), and induction. The enzymatic intrinsic clearance (Eq. 19 for the liver and Eq. 20 for the gut) needs to be modified accordingly:[52]

$$\sum_{j=1}^{J} \left(\sum_{i=1}^{I} \left(\left(\frac{V_{max_{E,x,j,i}} * [Sub]}{K_{m_{E,x,j,i}} * \left(1 + \sum_{c=1}^{C} \frac{[Inh]_c}{Ki_c}\right) + [Sub]} \right) \right) * ABt_{E,x,j} \right) \quad (25)$$

where [Sub] represents the substrate concentration, [Inh] is the concentration of the *c*th competitive inhibitor, Ki stands for the inhibition constant, ABt is the time-dependent enzyme abundance, and the subscript x represents either the liver or the gut. In the case of mechanism-based inhibition or induction, the enzyme concentration changes with time. The basal state can be described by ref. 52:

$$\frac{dABt_E}{dt} = k_{deg,E} * AB_E - k_{deg,E} * ABt_E = k_{deg,E} * (AB_{cyp} - ABt_{cyp}) \quad (26)$$

where k_{deg} represents the degradation rate. It holds that ABt(0) = AB. In the case of mechanism-based inhibition, Eq. 26 changes as follows[52]:

$$\frac{dABt_E}{dt} = k_{deg,E} * AB_E - \left(k_{deg,E} + \sum_{m=1}^{M} \frac{k_{inact,E,m} * [Inh]_m}{K_{app,E,m} + [Inh]_m} \right) * ABt_E \quad (27)$$

where k_{inact} and K_{app} are the inactivation rate of an enzyme and the apparent enzyme inhibition constant of the *m*th mechanism-based inhibitor. In the case of induction, the syntheses rate changes as follows[52]:

$$\frac{dABt_E}{dt} = k_{deg,E} * AB_E * \left(1 + \sum_{i=1}^{I} \frac{IndMax_{E,i} * [Inh]_i}{IC_{50,E,i} + [Inh]_i} \right) - k_{deg,E} * ABt_E \quad (28)$$

where IndMax and IC_{50} are the maximum fold of induction and the half maximal inducer concentration of the *i*th inducer. All DDI mechanisms are accounted for in Eq. 25.

Step 4: Bridge system and drug data—the ODE solver

After generating the population and drugs to inform the PBPK model, the ODEs are set up. ODEs are solved for each individual (ind) and each dose event (n) by the build-in stiff ODE solver ode15s[53] to ensure efficient running times of the code:

```
function[] = Solve ODE()

%This function solves the ordinary
differential equations

Convert variables from global to local

Calculate the number of ODE equations
Get the number of simulated timepoints
Get the number of simulated timepoints for
each dosing event

Initialize a vector for the simulated
timepoints
Initialize a matrix for the simulated
concentration

Run the ODE system for each virtual
individual separately
    Set the initial concentration for the
    first / single dose

    Run the ODE system for each dosing
    event separately
        Set the initial concentration for
        multiple dosing events
        Solve the ODEs

        Generate time steps for each
        dosing event with the user-defined
        resolution
        Evaluate the solution from the ODE
        system for each given timepoint

        Combine timepoints for each dosing
        event in the time vector
        Combine concentrations for each
        dosing event
    end
end

end
```

The function defining the initial concentration C0 for single doses and M0 for multiple dosing events needs to consider the drug concentration in a compartment at the timepoint of the *n*th multiple dose and is given by:

```
function C0 = Initialize_C();
    Set the initial concentration of each
    compartment to zero

    Set the initial CYP abundance in the
    liver and intestine according to [54,55]

    Define a case for each drug
        switch the route of administration
        for each drug
            in case the route of
            administration is an iv bolus
                then venous blood
                concentration is the dose
                divided by the venous volume
            in case the route of
            administration is oral
                then stomach concentration
                is the dose divided by the
                stomach volume
        end
    end
end
function M0 = Initialize_M(C0)
    if the first dose is administered
        then M0 has been defined by C0

    else
        M0 is defined by the calculated
        concentration of the last dosing
        event

    Define a case for each drug
        switch the route of administration
        for each drug
            in case the route of
            administration is an iv
            bolus
                dose divided by the
                venous volume is added to
                the venous conc.
            in case the route of
            administration is oral
                dose divided by the
                stomach volume is added
                to the stomach conc.
        end
    end
end
```

A relevant element is to define the right-hand site (rhs) of the differential equations to describe the drug movement from and to each compartment. The differential equations can be written as follows for the vascular, interstitial, and intracellular spaces of a generic compartment:

$$\frac{dc_{vas,org}}{dt} = \frac{1}{V_{vas,org}} * \left[Q_{org} * C_{ab} - (Q_{org} - L_{org}) * C_{vas,org} - J_{vas,org} * \left(\frac{C_{vas,org}}{BP} \right) + J_{ine,org} * C_{ine,org} \right], \tag{29}$$

$$\frac{dc_{ine,org}}{dt} = \frac{1}{V_{ine,org}} * \left[J_{vas,org} * \left(\frac{C_{vas,org}}{BP} \right) - J_{ine,org} * C_{ine,org} - L_{org} * C_{ine,org} - J_{in,org} * C_{ine,org} * fu_{ine,org} + J_{out,org} * C_{cel,org} * fu_{cel,org} \right], \tag{30}$$

$$\frac{dc_{cel,org}}{dt} = \frac{1}{V_{cel,org}} * \left[J_{in,org} * C_{ine,org} * fu_{ine,org} - J_{out,org} * C_{cel,org} * fu_{cel,org} \right] \tag{31}$$

where Q is the blood flow, L is the lymph flow, J is a flux, and the subscript ab represents the arterial blood pool. The Matlab function defining the rhs of the differential Eqs. 29–31 is written in the following way:

```
function dtdy = rhs(~, y)
        initialize the output as a column
        vector containing only zeros

        define subcompartments by a number

        write the differential equations
end
```

Some organs require a more detailed differential equation than the generic equations described in Eqs. 29–31. Blood flows from the venous blood pool into the lungs and after being loaded with oxygen, the blood returns to the arterial blood pool. Therefore, the differential equation of the vascular space of the lungs is given by:

$$\frac{dc_{vas,LU}}{dt} = \frac{1}{V_{vas,LU}} * \left[CO * C_{vb} - (CO - L_{LU}) * C_{vas,LU} - J_{vas,LU} * \left(\frac{C_{vas,LU}}{BP} \right) + J_{ine,LU} * C_{ine,LU} \right] \tag{32}$$

where CO is the cardiac output, and the subscripts LU and vb represent the lung and the venous blood pool, respectively.

In the kidney, the CL_R should be considered. A mechanistic kidney model including renal transporters is not described in this tutorial.

$$\frac{dc_{vas,KI}}{dt} = \frac{1}{V_{vas,KI}} * \left[Q_{KI} * C_{ab} - (Q_{KI} - L_{KI}) * C_{vas,KI} - J_{vas,KI} * \left(\frac{C_{vas,KI}}{BP} \right) J_{ine,KI} * C_{ine,KI} - CL_R * C_{vas,KI} * \frac{fu_{PL}}{BP} \right] \tag{33}$$

where the subscript KI stands for the kidney.

In the liver, active drug transporters and hepatic metabolism by enzymes are included and given by:

$$\frac{dc_{vas,LI}}{dt} = \frac{1}{V_{vas,LI}} * \Big[Q_{ha} * C_{ab} + Q_{PVBY} * C_{ab} + (Q_{GU} - L_{GU})$$
$$* C_{vas,GU} + Q_{SP} * C_{vas,SP} + (Q_{PA} - L_{PA})$$
$$* C_{vas,PA} - (Q_{LI} - L_{LI}) * C_{vas,LI} - J_{vas,LI}$$
$$* \Big(\frac{C_{vas,LI}}{BP}\Big) + J_{ine,LI} * C_{ine,LI} \Big], \tag{34}$$

$$\frac{dc_{ine,LI}}{dt} = \frac{1}{V_{ine,LI}} * \Big[J_{vas,LI} * \Big(\frac{C_{vas,LI}}{BP}\Big) - J_{ine,LI} * C_{ine,LI} - L_{LI}$$
$$* C_{ine,LI} - J_{in,LI} * C_{ine,LI} * fu_{ine,LI} + J_{out,LI}$$
$$* C_{cel,LI} * fu_{cel,LI} - \sum_{u=1}^{m} \Big(\frac{V_{max,up,hep,u} * C_{ine,LI} * fu_{ine,LI}}{K_{m,up,hep,u} + C_{ine,LI} * fu_{ine,LI}} + CL_{int,up,hep,u}$$
$$* C_{ine,LI} * fu_{ine,LI} \Big) * AB_{up,hep,u} * HPGL * W_{LI}$$
$$+ \sum_{e=1}^{m} \Big(\frac{V_{max,eff,hep,e} * C_{cel,LI} * fu_{cel,LI}}{K_{m,eff,hep,e} + C_{cel,LI} * fu_{cel,LI}} + CL_{int,eff,hep,e} * C_{ine,LI} * fu_{ine,LI} \Big)$$
$$* AB_{eff,hep,e} * HPGL * W_{LI} \Big], \tag{35}$$

$$\frac{dc_{cel,org}}{dt} = \frac{1}{V_{cel,org}} * \Big[J_{in,LI} * C_{ine,LI} * fu_{ine,LI} - J_{out,LI} * C_{cel,LI} * fu_{cel,LI}$$
$$+ \sum_{u=1}^{m} \Big(\frac{V_{max,up,hep,u} * C_{int,LI} * fu_{int,LI}}{K_{m,up,hep,u} + C_{int,LI} * fu_{int,LI}} + CL_{int,up,hep,u} * C_{ine,LI} * fu_{ine,LI} \Big)$$
$$* AB_{up,hep,u} * HPGL * W_{LI} - \sum_{e=1}^{m} \Big(\frac{V_{max,eff,hep,e} * C_{cel,LI} * fu_{cel,LI}}{K_{m,eff,hep,e} + C_{cel,LI} * fu_{cel,LI}} + CL_{int,eff,hep,e} * C_{ine,LI} * fu_{ine,LI} \Big)$$
$$* AB_{eff,hep,e} * HPGL * W_{LI}$$
$$- \Big[\sum_{j=1}^{J} \Big(\sum_{i=1}^{I} \Big(\frac{V_{max,E,hep,j,i}}{K_{m,E,hep,j,i} * (1 + \Sigma[Inh]/Ki) + C_{cel,LI} * fu_{cel,LI}} + CL_{int,E,hep,j,i} \Big) * ABt_{E,hep,j} \Big) + CL_{int,hep} \Big] * MPPGL * W_{LI} * C_{cel,LI} \Big] \tag{36}$$

where HPGL is the hepatocellularity, and the subscripts LI, ha, PVBY, GU, SP, PA, up, and eff represent the liver, hepatic arterial, portal vein bypass, gut, spleen, pancreas, uptake, and efflux, respectively.

Lymph fluid flows through afferent lymph vessels from the interstitial space of organs to the central lymph-node compartment and further to the venous blood pool, given by:

$$\frac{dc_{vas,LN}}{dt} = \frac{1}{V_{vas,LN}} * [Q_{LN} * (C_{ab} - C_{vas,LN}) + L_{tot}$$
$$* (C_{ine,LN} - C_{vas,LN})], \tag{37}$$

$$\frac{dc_{ine,LN}}{dt} = \frac{1}{V_{ine,LN}} * \Big[\sum_{org=1}^{O} (L_{org} * C_{ine,org}) - L_{tot} * C_{ine,LN} - J_{in,LN}$$
$$* C_{ine,LN} * fu_{ine,LN} + J_{out,LN} * C_{cel,LN} * fu_{cel,LN} \Big] \tag{38}$$

where L_{tot} is the total lymph flow, and the subscript LN represents the central lymph-node compartment.

The differential equations for the venous and arterial blood compartments are given by:

$$\frac{dc_{vb}}{dt} = \frac{1}{V_{vb}} * \Big[C_{vas,AD} * (Q_{AD} - L_{AD}) + C_{vas,BO} * Q_{BO} + C_{vas,BR}$$
$$* (Q_{BR} - L_{BR}) + C_{vas,GO} * (Q_{GO} - L_{GO}) + C_{vas,HE}$$
$$* (Q_{HE} - L_{HE}) + C_{vas,KI} * (Q_{KI} - L_{KI}) + C_{vas,MU}$$
$$* (Q_{MU} - L_{MU}) + C_{vas,SK} * (Q_{SK} - L_{SK}) + C_{vas,TH}$$
$$* (Q_{TH} - L_{TH}) + C_{vas,LI} * (Q_{LI} - L_{LI}) + C_{vas,LN}$$
$$* (Q_{LN} + L_{tot}) + C_{vas,RE} * (Q_{RE} - L_{RE}) - CO * C_{vb} \Big], \tag{39}$$

$$\frac{dc_{ab}}{dt} = \frac{1}{V_{ab}} * \Big[(CO - L_{LU}) * C_{vas,LU}$$
$$- \sum_{o=1}^{O} (Q_{org,o} * C_{ab}) - CL_{ad} * C_{ab} * \frac{fu_{PL}}{BP} \Big] \tag{40}$$

where the subscripts AD, BO, BR, GO, HE, MU, SK, TH, and RE represent adipose, bone, brain, gonads, heart, muscle, skin, thymus, and remaining organ, respectively.

The solution of the different equation needs to be evaluated in Matlab using the implemented *deval* function over a predefined number of timepoints (*NumPoints*). The solution for the drug concentration of each compartment is saved in the matrix *Conc*, and the corresponding timepoint to the concentration is saved in the vector *Time* as described previously.

Step 5: Work with the simulated data—the postprocessing step

The solution of the differential equation solver has been saved into one single matrix. The first step of postprocessing is therefore to extract the concentration for each compartment of the model from the solution matrix of the ODE solver. Different statistics can now be calculated with the extracted concentrations, such as the mean and the 5 and 95 percentiles with predefined Matlab commands, which require the Statistics and Machine Learning Toolbox as an add-on to the Matlab suite.

One important aspect of postprocessing is to ensure mass balance of the model. The concentration of each compartment is multiplied by the compartmental volume, and the drug amount cleared by a specific pathway as well as the amount not being absorbed are integrated and added together. The product should be equivalent to the dose entered in the study design.

Pharmacokinetic parameters, such as the maximal concentration (C_{max}), the timepoint of the maximal concentration (T_{max}), the area under the curve (AUC), the apparent clearance (CL/F), and the apparent volume of distribution (VD/F) can be calculated for each compartment. The elimination rate is used to extrapolate the AUC to infinity and to calculate the clearance and the volume of distribution.

```
function[] = PostProcessing()

%This function processes the data from the
ODE solution and outputs the results
%Attention: Some statistical calculations
(geomean, prctile) require
```
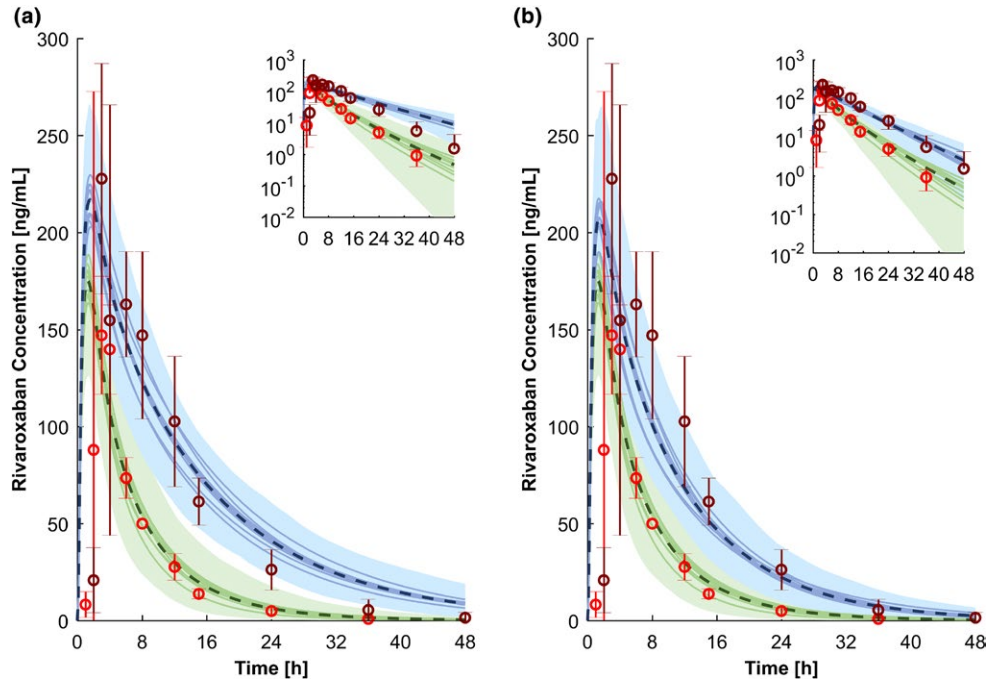
Figure 5 Physiologically-based pharmacokinetic simulations for a single dose of 10 mg rivaroxaban administered with 600 mg ritonavir twice daily in steady state (**a**) and 800/100 mg darunavir/ritonavir once daily in steady state (**b**). Green represents the prediction of rivaroxaban alone, and blue shows the prediction of rivaroxaban administered with the perpetrators. The dashed line and the shaded area are the mean and the 95% confidence interval for the prediction of all virtual individuals, respectively. The solid lines show the mean of each virtual trial (10 trials with 12 virtual subjects per trial have been simulated). The red and the dark red circles show the observed clinical data of 10 mg rivaroxaban alone and coadministered with 600 mg ritonavir twice daily.[57] Conc., concentration; h, hour.

```
%the Statistical and Machine Learning
Toolbox

Initialize Cmax
Initialize Tmax
Initialize AUCt

Calculate PK parameters for each simulated
drug
    Calculate PK parameters for each virtual
    individual
        if the venous concentration at
        timepoint t is bigger than Cmax
            than the venous concentration at
            timepoint t is the new Cmax
            than the timepoint t is the new
            Tmax
        end

        Calculate the AUC according to the
        linear trapezoidal rule
    end
end


take the logarithm of the concentration for
extrapolation

Initialize the slope and beta

Calculate the slope and beta for each
simulated drug
    Calculate the slope and beta for each
    virtual individual
        linear regression of the last four
        timepoints
            beta is the slope of the
            regression
    end
end
LogVenousConc = log10(VenousConc);

half-life is the natural logarithm of two
divided by beta
AUC extrapolated to infinity is the AUCt
plus the venous concentration at the last
simulated timepoint divided by beta
Clearance is the dose divided by the AUC
extrapolated to infinity
Volume of distribution is the clearance
divided by beta

end
```

As shown above for the concentration, the mean and percentiles or other statistics can be calculated for pharmacokinetic parameters.

Table 2 Observed vs. predicted pharmacokinetic parameters

Pharmacokinetic parameter	C_{max} (ng/mL)		T_{max} (h)		AUC (ng × h/mL)		$t_{1/2}$ (h)	
	Observed	Predicted	Observed	Predicted	Observed	Predicted	Observed	Predicted
Rivaroxaban 10 mg	153.7 ± 23.7	162.7 ± 26.9	3.0 ± 0.5	1.5 ± 0.1	1,000 ± 161	1,208 ± 268	5.7 ± 1.8	12.5 ± 3.3
Rivaroxaban 10 mg + Ritonavir 600 mg twice daily	238.0 ± 55.7	197.4 ± 32.6	4.0 ± 2.2	1.6 ± 0.2	2,529 ± 425	2,761 ± 875	6.9 ± 2.2	20.2 ± 4.7
Ratio	1.55 ± 0.43	1.21 ± 0.28	1.33 ± 0.77	1.09 ± 0.14	2.53 ± 0.59	2.29 ± 0.88	1.21 ± 0.53	1.62 ± 0.57
Rivaroxaban 10 mg + Darunavir/r 800/100 mg once daily	NA	190.0 ± 31.2	NA	1.7 ± 0.2	NA	2,510 ± 685	NA	19.9 ± 5.2
Ratio	NA	1.17 ± 0.27	NA	1.16 ± 0.15	NA	2.08 ± 0.73	NA	1.60 ± 0.60
Darunavir/r 800/100 mg once daily	6,803 ± 1,618	5,432 ± 1,929	3.6 ± 1.6	3.1 ± 0.5	75,780 ± 22,102	75,002 ± 56,887	14.4 ± 5.2	10.9 ± 5.7
Ritonavir 100 mg once daily	606 ± 281	531 ± 280	3.1 ± 2.0	1.8 ± 0.5	5,296 ± 4,664	5,470 ± 3,132	6.3 ± 1.5	5.4 ± 1.4

Data are presented as mean +/- standard deviation. Observed data are published in ref. 57 for rivaroxaban, refs. 58–60 for darunavir, and refs.59,61 for ritonavir.

C_{max}, maximal concentration; T_{max}, timepoint of the maximal concentration; AUC, area under the curve; t1/2 = elimination half-life; NA = not applicable.
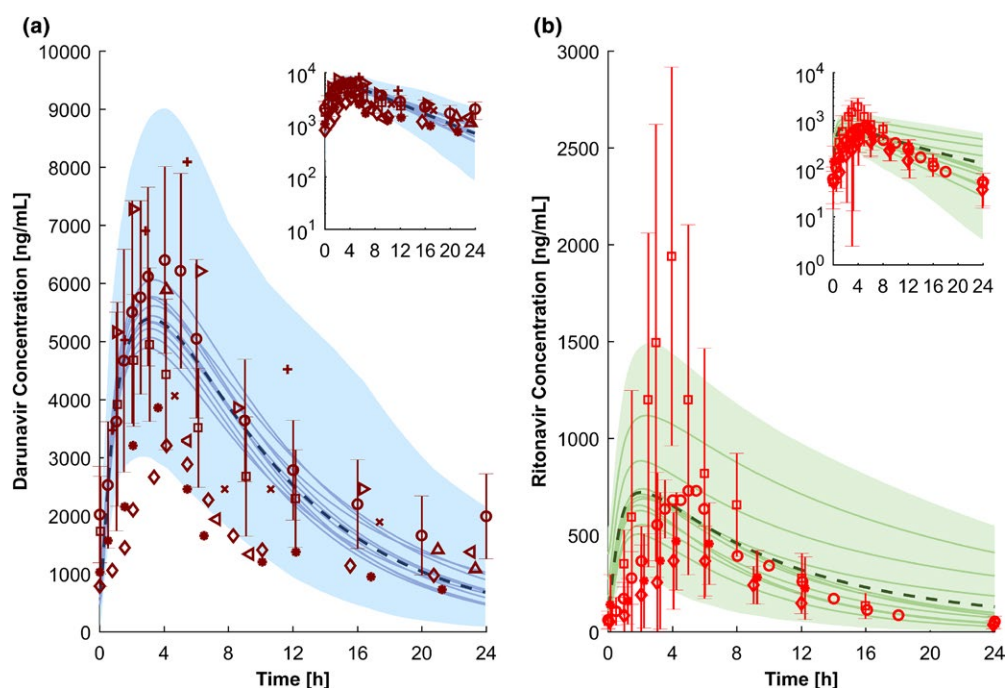

Figure 6 Physiologically-based pharmacokinetic simulations for 800 mg darunavir once daily boosted with 100 mg ritonavir once daily (**a**) and 100 mg ritonavir once daily (**b**). The dashed line and the shaded area are the mean and the 95% confidence interval for the prediction of all virtual individuals, respectively. The solid lines how the mean of each virtual trial (10 trials with 12 virtual subjects per trial have been simulated). The red markers show observed clinical data (**a**: refs. 58–60; **b**: refs. 59,61,62). Conc., concentration; h, hour.

The results can be either output graphically using the built-in *plot* function or can be exported to Excel (Microsoft, Redmond, WA) using the *xlswrite* command.

SIMULATION OF THE DDI MAGNITUDE BETWEEN RIVAROXABAN AND DARUNAVIR/RITONAVIR

To illustrate the steps of PBPK model development, the DDI magnitude between a single dose of rivaroxaban and darunavir boosted with ritonavir under steady-state conditions will

be simulated. The rivaroxaban PBPK model was developed combining published *in vitro* data (bottom-up approach) with clinical clearance data (top-down approach). Validated PBPK models for darunavir and ritonavir were used.[56] Ritonavir has an impact on the CL_R of rivaroxaban,[57] which was considered in the model. The parameters of the drug models can be found in the model code (**Supplementary Material S1**). A clinical DDI investigating the effect of 600 mg ritonavir twice daily on a single 10 mg dose of oral rivaroxaban in 12 healthy men aged 18–44 years was used to

verify the rivaroxaban model.[57] A total of 10 virtual trials with 12 men (proportion of women is set to zero) aged 20–44 years were simulated. Afterward, the effect of 800/100 mg darunavir/ritonavir once daily (qd) on a single oral dose of 10 mg rivaroxaban was simulated because the boosted protease inhibitor is given in clinical practice.

The simulation of 10 mg rivaroxaban with and without 600 mg of oral ritonavir were in good agreement with the observed clinical data (**Figure 5a**). T_{max} of rivaroxaban was underpredicted by twofold because T_{max} was achieved 1.5 hours later in the clinical study compared with the simulation. However, the predicted T_{max} ratio of rivaroxaban administered with 600 mg ritonavir twice daily and rivaroxaban given without a perpetrator was within 1.25-fold of the observed data. The elimination half-life of rivaroxaban was overpredicted by twofold, but C_{max} and AUC were predicted within 1.25-fold (bioequivalence criterion; **Table 2**). The effect of 100 mg ritonavir qd used to boost darunavir in clinical practice is predicted to be similar to 600 mg of ritonavir twice daily (**Figure 5b**) because full inhibition of CYP CYP3A4 and CYP2J2 is already achieved.

The predicted concentrations of the two perpetrators darunavir (800 mg qd) and ritonavir (100 mg qd) are in accordance with observed clinical data from various studies (**Figure 6**). The T_{max} of ritonavir was underpredicted by twofold, but all pharmacokinetic parameters of boosted darunavir and ritonavir were within the 1.25-fold interval of the observed clinical data (**Table 2**).

CONCLUSION

We have described a comprehensive strategy to develop and code a PBPK model in Matlab with potential applications in other pharmacological scenarios. Of interest, PBPK models are increasingly accepted for the prediction of DDIs and drug disposition in special populations such as pediatrics and the elderly. Furthermore, this type of computational framework can be integrated with pharmacodynamic models, which can be easily added to custom build PBPK models in Matlab.

Supporting Information. Supplementary information accompanies this paper on the *CPT: Pharmacometrics & Systems Pharmacology* website (www.psp-journal.com).

Table S1. Parameters and their abbreviation and units used to build a physiologically-based pharmacokinetic model.
Table S2. Subscripts and their abbreviation used to build the physiologically-based pharmacokinetic model.
Supplementary Material S1. Model code.

Conflict of Interest. The authors declared no competing interests for this work.

1. Jamei, M. Recent advances in development and application of physiologically-based pharmacokinetic (PBPK) models: a transition from academic curiosity to regulatory acceptance. *Curr. Pharmacol. Rep.* **2**, 161–169 (2016).

2. U.S. Food and Drug Administration. Physiologically based pharmacokinetic analysis – format and content. Guidance for industry <https://www.fda.gov/downloads/Drugs/GuidanceComplianceRegulatoryInformation/Guidances/UCM531207.pdf> (2016). Accessed January 2, 2018.

3. European Medicines Agency. Guideline on the qualification and reporting of physiologically based pharmacokinetic (PBPK) modelling and simulation <http://www.ema.europa.eu/docs/en_GB/document_library/Scientific_guideline/2016/07/WC500211315.pdf> (2016). Accessed January 2, 2018.

4. Rowland-Yeo, K., Jamei, M. & Rostami-Hodjegan, A. Predicting drug–drug interactions: application of physiologically based pharmacokinetic models under a systems biology approach. *Expert Rev. Clin. Pharmacol.* **6**, 143–157 (2013).

5. Stader, F., Würthwein, G., Groll, A.H., Vehreschild, J.J., Cornely, O.A. & Hempel, G. Physiology-based pharmacokinetics of caspofungin for adults and paediatrics. *Pharm. Res.* **32**, 2029–2037 (2015).

6. Ke, A.B., Nallani, S., Zhao, P., Rostami-Hodjegan, A., Isoherranen, N. & Unadkat, J.D. A PBPK model to predict disposition of P450 2D6 and P450 1A2 metabolized drugs in pregnant women. *Drug Metab. Dispos.* **41**, 801–813 (2013).

7. Olagunju, A., Rajoli, R.K., Atoyebi, S.A., Khoo, S., Owen, A. & Siccardi, M. Physiologically-based pharmacokinetic modelling of infant exposure to efavirenz through breastfeeding. *AAS Open Res.* **1**, 1–16 (2018).

8. Johnson, T.N., Boussery, K., Rowland-Yeo, K., Tucker, G.T. & Rostami-Hodjegan, A. A semi-mechanistic model to predict the effects of liver cirrhosis on drug clearance. *Clin. Pharmacokinet.* **49**, 189–206 (2010).

9. Rowland Yeo, K., Aarabi, M., Jamei, M. & Rostami-Hodjegan, A. Modeling and predicting drug pharmacokinetics in patients with renal impairment. *Expert Rev. Clin. Pharmacol.* **4**, 261–274 (2011).

10. Rajoli, R.K. *et al.* Physiologically based pharmacokinetic modelling to inform development of intramuscular long-acting nanoformulations for HIV. *Clin. Pharmacokinet.* **54**, 639–650 (2015).

11. Schmitt, W. & Willmann, S. Physiology-based pharmacokinetic modeling: ready to be used. *Drug Discov. Today Technol.* **1**, 449–456 (2004).

12. Edginton, A.N., Theil, F.-P., Schmitt, W. & Willmann, S. Whole body physiologically-based pharmacokinetic models: their use in clinical drug development. *Expert Opin. Drug Metab. Toxicol.* **4**, 1143–1152 (2008).

13. Stader, F., Siccardi, M., Battegay, M., Kinvig, H., Penny, M.A. & Marzolini, C. Repository describing an aging population to inform physiologically based pharmacokinetic models considering anatomical, physiological, and biological age-dependent changes. *Clin. Pharmacokinet.* **58**(4), 483–501 (2019).

14. Jamei, M., Dickinson, G.L. & Rostami-Hodjegan, A. A framework for assessing inter-individual variability in pharmacokinetics using virtual human populations and integrating general knowledge of physical chemistry, biology, anatomy, physiology and genetics: a tale of 'bottom-up' vs 'top-down' recognition of covariates. *Drug Metab. Pharmacokinet.* **24**, 53–75 (2009).

15. Barton, H.A. *et al.* Characterizing uncertainty and variability in physiologically based pharmacokinetic models: state of the science and needs for research and implementation. *Toxicol. Sci.* **99**, 395–402 (2007).

16. Khalil, F. & Läer, S. Physiologically based pharmacokinetic modeling: methodology, applications, and limitations with a focus on its role in pediatric drug development. *Biomed. Res. Int.* **2011**, 1–13 (2011).

17. Howgate, E., Rowland Yeo, K., Proctor, N., Tucker, G. & Rostami-Hodjegan, A. Prediction of in vivo drug clearance from in vitro data. I: impact of inter-individual variability. *Xenobiotica* **36**, 473–497 (2006).

18. Jamei, M., Marciniak, S., Feng, K., Barnett, A., Tucker, G. & Rostami-Hodjegan, A. The Simcyp® population-based ADME simulator. *Expert Opin. Drug Metab. Toxicol.* **5**, 211–223 (2009).

19. Willmann, S., Lippert, J., Sevestre, M., Solodenko, J., Fois, F. & Schmitt, W. PK-Sim®: a physiologically based pharmacokinetic 'whole-body' model. *Biosilico* **1**, 121–124 (2003).

20. Gastro Plus. Product of simulations plus <www.simulationsplus.com>. Accessed January 2, 2018.

21. Johnson, T.N., Rostami-Hodjegan, A. & Tucker, G.T. Prediction of the clearance of eleven drugs and associated variability in neonates, infants and children. *Clin. Pharmacokinet.* **45**, 931–956 (2006).

22. Jones, H. & Rowland-Yeo, K. Basic concepts in physiologically based pharmacokinetic modeling in drug discovery and development. *CPT Pharmacometrics Syst. Pharmacol.* **2**, 1–12 (2013).

23. Pomerantz, R.J. Reservoirs of human immunodeficiency virus type 1: the main obstacles to viral eradication. *Clin. Infect. Dis.* **34**, 91–97 (2002).

24. Emami Riedmaier, A., Burt, H., Abduljalil, K. & Neuhoff, S. More power to OATP1B1: an evaluation of sample size in pharmacogenetic studies using a rosuvastatin PBPK model for intestinal, hepatic, and renal transporter-mediated clearances. *J. Clin. Pharmacol.* **56**(S7), S132–S142 (2016).

25. Yu, L.X. & Amidon, G.L. A compartmental absorption and transit model for estimating oral drug absorption. *Int. J. Pharm.* **186**, 119–125 (1999).

26. Jamei, M. *et al.* Population-based mechanistic prediction of oral drug absorption. *AAPS J.* **11**, 225–237 (2009).

27. Darwich, A., Neuhoff, S., Jamei, M. & Rostami-Hodjegan, A. Interplay of metabolism and transport in determining oral drug absorption and gut wall metabolism: a simulation assessment using the "Advanced Dissolution, Absorption, Metabolism (ADAM)" model. *Curr. Drug Metab.* **11**, 716–729 (2010).

28. Estudante, M., Morais, J.G., Soveral, G. & Benet, L.Z. Intestinal drug transporters: an overview. *Adv. Drug Deliv. Rev.* **65**, 1340–1356 (2013).

29. Sun, D. *et al.* Comparison of human duodenum and Caco-2 gene expression profiles for 12,000 gene sequences tags and correlation with permeability of 26 drugs. *Pharm. Res.* **19**, 1400–1416 (2002).

30. Helander, H.F. & Fändriks, L. Surface area of the digestive tract–revisited. *Scand. J. Gastroenterol.* **49**, 681–689 (2014).

31. Valentin, J. Basic anatomical and physiological data for use in radiological protection: reference values: ICRP Publication 89. *Ann. ICRP* **32**, 1–277 (2002).

32. Sugano, K. Artificial membrane technologies to assess transfer and permeation of drugs in drug discovery. *Compr. Med. Chem. II* **5**, 453–487 (2007).

33. Crowe, P.T. & Marsh, M.N. Morphometric analysis of small intestinal mucosa IV. Determining cell volumes. *Virchows Arch.* **422**, 459–466 (1993).

34. Gill, K.L., Gardner, I., Li, L. & Jamei, M. A bottom-up whole-body physiologically based pharmacokinetic model to mechanistically predict tissue distribution and the rate of subcutaneous absorption of therapeutic proteins. *AAPS J.* **18**, 156–170 (2016).

35. Wasan, K.M. The role of lymphatic transport in enhancing oral protein and peptide drug delivery. *Drug Dev. Ind. Pharm.* **28**, 1047–1058 (2002).

36. Poulin, P. & Theil, F.P. Prediction of pharmacokinetics prior to in vivo studies. 1. Mechanism-based prediction of volume of distribution. *J. Pharm. Sci.* **91**, 129–156 (2002).

37. Poulin, P. & Theil, F.P. Prediction of pharmacokinetics prior to in vivo studies. 2. Generic physiologically based pharmacokinetic models of drug disposition. *J. Pharm. Sci.* **91**, 1358–1370 (2002).

38. Rodgers, T., Leahy, D. & Rowland, M. Physiologically based pharmacokinetic modeling. 1. Predicting the tissue distribution of moderate-to-strong bases. *J. Pharm. Sci.* **94**, 1259–1276 (2005).

39. Rodgers, T. & Rowland, M. Physiologically based pharmacokinetic modelling. 2. Predicting the tissue distribution of acids, very weak bases, neutrals and zwitterions. *J. Pharm. Sci.* **95**, 1238–1257 (2006).

40. Rodgers, T. & Rowland, M. Mechanistic approaches to volume of distribution predictions: understanding the processes. *Pharm. Res.* **24**, 918–933 (2007).

41. Schmitt, W. General approach for the calculation of tissue to plasma partition coefficients. *Toxicol. In Vitro* **22**, 457–467 (2008).

42. Rippe, B. & Haraldsson, B. Fluid and protein fluxes across small and large pores in the microvasculature. Application of two-pore equations. *Acta Physiol. Scand.* **131**, 411–428 (1987).

43. Burt, H.J., Riedmaier, A.E., Harwood, M.D., Crewe, H.K., Gill, K.L. & Neuhoff, S. Abundance of hepatic transporters in Caucasians: a meta-analysis. *Drug Metab. Dispos.* **44**, 1550–1561 (2016).

44. Tachibana, T., Kato, M., Takano, J. & Sugiyama, Y. Predicting drug-drug interactions involving the inhibition of intestinal CYP3A4 and P-glycoprotein. *Curr. Drug Metab.* **11**, 762–777 (2010).

45. Jamei, M. *et al.* A mechanistic framework for in vitro–in vivo extrapolation of liver membrane transporters: prediction of drug–drug interaction between rosuvastatin and cyclosporine. *Clin. Pharmacokinet.* **53**, 73–87 (2014).

46. Noé, J., Portmann, R., Brun, M.-E. & Funk, C. Substrate-dependent drug-drug interactions between gemfibrozil, fluvastatin and other organic anion-transporting peptide (OATP) substrates on OATP1B1, OATP2B1, and OATP1B3. *Drug Metab. Dispos.* **35**, 1308–1314 (2007).

47. Rostami-Hodjegan, A. & Tucker, G. 'In silico' simulations to assess the 'in vivo' consequences of 'in vitro' metabolic drug–drug interactions. *Drug Discov. Today Technol.* **1**, 441–448 (2004).

48. Pang, K.S. & Rowland, M. Hepatic clearance of drugs. I. Theoretical considerations of a "well-stirred" model and a "parallel tube" model. Influence of hepatic blood flow, plasma and blood cell binding, and the hepatocellular enzymatic activity on hepatic drug clearance. *J. Pharmacokinet. Biopharm.* **5**, 625–653 (1977).

49. Neuhoff, S. *et al.* Accounting for transporters in renal clearance: towards a mechanistic kidney model (Mech KiM). In *Transporters in Drug Development* (ed. Sugiyama, Y, Steffansen, B.) 155–177 (Springer Nature Switzerland AG, Gewerbestrasse 11 6330 Cham Switzerland, 2013).

50. Edginton, A.N., Schmitt, W., Voith, B. & Willmann, S. A mechanistic approach for the scaling of clearance in children. *Clin. Pharmacokinet.* **45**, 683–704 (2006).

51. Cubitt, H.E., Rowland-Yeo, K., Howgate, E.M., Rostami-Hodjegan, A. & Barter, Z.E. Sources of interindividual variability in IVIVE of clearance: an investigation into the prediction of benzodiazepine clearance using a mechanistic population-based pharmacokinetic model. *Xenobiotica* **41**, 623–638 (2011).

52. Almond, L.M. *et al.* Prediction of drug-drug interactions arising from CYP3A induction using a physiologically based dynamic model. *Drug Metab. Dispos.* **44**, 821–832 (2016).

53. Shampine, L.F. & Reichelt, M.W. The Matlab ode suite. *SIAM J. Sci. Comput.* **18**, 1–22 (1997).

54. Achour, B., Russell, M.R., Barber, J. & Rostami-Hodjegan, A. Simultaneous quantification of the abundance of several cytochrome P450 and uridine 5′-diphospho-glucuronosyltransferase enzymes in human liver microsomes using multiplexed targeted proteomics. *Drug Metab. Dispos.* **42**, 500–510 (2014).

55. Paine, M.F. *et al.* Characterization of interintestinal and intraintestinal variations in human CYP3A-dependent metabolism. *J. Pharmacol. Exp. Ther.* **283**, 1552–1562 (1997).

56. Moltó, J. *et al.* Use of a physiologically based pharmacokinetic model to simulate drug–drug interactions between antineoplastic and antiretroviral drugs. *J. Antimicrob. Chemother.* **72**, 805–811 (2016).

57. Mueck, W., Kubitza, D. & Becka, M. Co-administration of rivaroxaban with drugs that share its elimination pathways: pharmacokinetic effects in healthy subjects. *Br. J. Clin. Pharmacol.* **76**, 455–466 (2013).

58. Kakuda, T.N. *et al.* Pharmacokinetics of darunavir in fixed-dose combination with cobicistat compared with coadministration of darunavir and ritonavir as single agents in healthy volunteers. *J. Clin. Pharmacol.* **54**, 949–957 (2014).

59. DeJesus, E. *et al.* Pharmacokinetics of once-daily etravirine without and with once-daily darunavir/ritonavir in antiretroviral-naive HIV type-1-infected adults. *Antivir. Ther.* **15**, 711 (2010).

60. Boffito, M., Miralles, D. & Hill, A. Pharmacokinetics, efficacy, and safety of darunavir/ritonavir 800/100 mg once-daily in treatment-naive and-experienced patients. *HIV Clin. Trials* **9**, 418–427 (2008).

61. Mathias, A., West, S., Hui, J. & Kearney, B. Dose-response of ritonavir on hepatic CYP3A activity and elvitegravir oral exposure. *Clin. Pharmacol. Ther.* **85**, 64–70 (2009).

62. Burger, D., Agarwala, S., Child, M., Been-Tiktak, A., Wang, Y. & Bertz, R. Effect of rifampin on steady-state pharmacokinetics of atazanavir with ritonavir in healthy volunteers. *Antimicrob. Agents Chemother.* **50**, 3336–3342 (2006).